



ACADEMIC  
PRESS

Available online at [www.sciencedirect.com](http://www.sciencedirect.com)

SCIENCE @ DIRECT®

Journal of Solid State Chemistry 176 (2003) 400–411

JOURNAL OF  
SOLID STATE  
CHEMISTRY

<http://elsevier.com/locate/jssc>

# Calculation of exchange coupling constants in solid state transition metal compounds using localized atomic orbital basis sets

Eliseo Ruiz,<sup>a,c</sup> Miquel Lluell,<sup>b,c</sup> and Pere Alemany<sup>b,c,\*</sup>

<sup>a</sup> *Departament de Química Inorgànica, Universitat de Barcelona, Diagonal 647, Barcelona 08028, Spain*

<sup>b</sup> *Departament de Química Física, Universitat de Barcelona, Diagonal 647, Barcelona 08028, Spain*

<sup>c</sup> *Centre Especial de Recerca en Química Teòrica (CERQT), Universitat de Barcelona, Diagonal 647, Barcelona 08028, Spain*

Received 24 January 2003; received in revised form 9 April 2003; accepted 24 April 2003

## Abstract

The application of theoretical methods based on density functional theory using hybrid functionals and localized, atomic orbital type basis sets is shown to provide good estimates for exchange coupling constants in non-metallic, solid state transition metal compounds with relatively complex crystal structures. The accuracy of the calculated exchange coupling constants is similar to that previously obtained for dinuclear and polynuclear molecular compounds. As an application of this procedure, the magnetic properties of the high-temperature phase of  $\text{CuGeO}_3$ , the recently synthesized silver copper oxide  $\text{Ag}_2\text{Cu}_2\text{O}_3$ , and the family of  $M[\text{N}(\text{CN})_2]_2$  ( $M = \text{Cr}(\text{II}), \text{Mn}(\text{II}), \text{Fe}(\text{II}), \text{Co}(\text{II}), \text{Ni}(\text{II})$  and  $\text{Cu}(\text{II})$ ) compounds are analyzed via the computation of their most relevant exchange coupling constants.

© 2003 Elsevier Inc. All rights reserved.

**Keywords:** Exchange coupling; Density functional theory; Transition metal compounds; Magnetic properties; Dicyanamides;  $\text{CuGeO}_3$

## 1. Introduction

Molecular magnetism is one of the most active areas in modern transition metal chemistry [1–4]. Early on, research in this field focused mainly on the magnetic properties of isolated dinuclear complexes with the aim of gaining some understanding of the key structural and electronic factors that control the exchange coupling between two metal centers bearing unpaired electrons. During the last decade, however, interest in molecular magnetism has shifted towards the preparation of new materials with more complex magnetic structures [5]. New magnetic properties have been sought for by extending the dimensionality of the exchange interaction to chain, two- or even three-dimensional structures based on molecular building blocks. The result of this effort is the synthesis of extended structures in which metal centers bearing unpaired electrons are linked by different bridging units giving rise to non-metallic materials with interesting magnetic properties. Follow-

ing the usual procedure adopted for molecular species, these magnetic properties are often interpreted in terms of a phenomenological Heisenberg Hamiltonian involving several exchange pathways that can be characterized by the corresponding exchange coupling constant for each pair of coupled paramagnetic units. Although fitting the magnetic susceptibility curves to obtain the value of the coupling constants is feasible for discrete, one- and two-dimensional systems, this procedure encounters some difficulties in the case of three-dimensional networks for which only approximate mean-field models are available for extracting the values of the coupling constants from experimental data [6].

From a theoretical point of view, the calculation of the exchange coupling constants of transition metal compounds has been limited usually to dinuclear complexes [7] although a few attempts to obtain this property for isolated polynuclear compounds [8] or even for extended solid state structures have been published recently [9,10]. The need for the inclusion of electron correlation effects to reach a proper description of the electronic structure of exchange coupled polynuclear transition metal compounds has limited the applications of the most popular semiempirical methods in this field

\*Corresponding author. Departament de Química Física, Universitat de Barcelona, Diagonal 647, Barcelona 08028, Spain.

E-mail address: [alemany@qf.ub.es](mailto:alemany@qf.ub.es) (P. Alemany).

[11]. Sophisticated post-Hartree–Fock methods have been shown to provide good approximations to coupling constants for molecular species, but the huge demand of computational resources associated to these methods severely limits their applicability to most of the complexes of actual experimental interest [12–14]. This approach is also only available in the case of extended solid state structures if the crystal structure is fragmented into isolated clusters containing a finite number of paramagnetic centers [15]. The calculation of exchange coupling constants for extended periodic structures has thus been attempted mainly using the UHF method that has been shown to provide only qualitative values in the case of dinuclear compounds where comparison with more sophisticated post-Hartree–Fock methods and accurate experimental data is possible [16,17]. The application of density functional theory (DFT) [18] based methods for the calculation of exchange coupling constants in dinuclear compounds has been shown in the last years to provide a reasonable compromise between the size of the compounds that can be studied and the accuracy of the calculated coupling constants that can be extracted from them [17,19–21]. Considering that these methods have also been implemented in programs designed for the calculation of the electronic structure of periodic systems [22], this approach offers the opportunity for studying extended solids at the same level as discrete molecular entities.

The comparison of calculated exchange coupling constants with those obtained experimentally is, however, not straightforward since experimental data are in most cases obtained from a fitting of the magnetic susceptibility to the expression obtained using a model that includes several simplifying assumptions. One of the problems associated with this technique is the existence of several independent sets of parameters that provide a reasonably good fitting of the susceptibility curve. Another difficulty arises because some simplifying hypothesis, such as the neglect of next-nearest neighbor interactions or the assumption of identical parameters for interactions that are not exactly equivalent by symmetry, are often adopted to reduce the number of fitting parameters. The situation is especially difficult for the case of three-dimensional networks for which no models relating the experimental data with the coupling constants are available and only approximate mean-field results relating the value of  $J$  to the critical temperature can be applied [6,23]. Thus, the use of theoretical methods to estimate the exchange coupling constants can be foreseen as a valuable tool for the experimentalist to rule out those sets of experimental fitted constants that are deemed unrealistic according to calculations.

The present paper has a principal goal, which is to show that the general strategy used to calculate exchange coupling constants for isolated polynuclear

transition metal compounds can be easily adapted to the determination of these parameters in extended solid state compounds. For this, we have used CRYSTAL98 [22], a general purpose program for the calculation of the electronic structure for periodic systems using localized, atomic basis sets which allows the option of performing spin-polarized calculations both at the Hartree–Fock and DFT levels including hybrid functionals. The applicability of the proposed method will be illustrated by applying it to three different examples for which partial experimental information is available.

## 2. Calculation of exchange coupling constants in dinuclear compounds

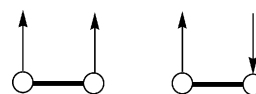
If we neglect the zero field splitting terms, the main parameter used to quantify the magnetic properties of a dinuclear complex is the exchange coupling constant  $J$  between the two paramagnetic centers with total spins  $S_1$  and  $S_2$ , respectively, which is defined through the phenomenological Heisenberg Hamiltonian:

$$\hat{H} = -J\hat{S}_1\hat{S}_2. \quad (1)$$

We have shown in previous works that methods based on DFT using hybrid functionals constitute a powerful tool to calculate exchange coupling constants, and hence magnetic properties, of dinuclear systems [19–21,24–28]. The estimation of the exchange coupling constant in a dinuclear compound involves the calculation of the energy difference between the high- and low-spin solutions shown schematically in Scheme 1. In the case of symmetric homodinuclear complexes the low-spin solution corresponds to a broken symmetry wavefunction [29–31]. Using the phenomenological spin Hamiltonian (Eq. (1)) for the simplest case of one unpaired electron on each of the two centers, it may be easily shown that the value of the exchange coupling constant corresponds to the energy difference between the triplet and the singlet states. We have shown in previous work [17] that when using DFT calculations the energy of the singlet state can be approximated using that of the single-determinant broken-symmetry solution shown in Scheme 1 and the relation between the calculated energies and the exchange coupling constant is

$$E_{BS} - E_{HS} = (2S_1S_2 + S_2)J_{12}, \quad (2a)$$

where  $S_2 \leq S_1$  are the spins on each paramagnetic center. On the other hand, for Hartree–Fock calculations a spin-projected formula must be used and the relationship



Scheme 1.

between the calculated energies and the exchange coupling constant that results is

$$E_{\text{BS}} - E_{\text{HS}} = 2S_1S_2J_{12}. \quad (2b)$$

The use of the non-spin projected energy of the broken symmetry solution as the energy of the low-spin state within the DFT framework has been the source of controversy between different authors [16,17,32]. Recently, Polo et al. have shown that the self-interaction error of commonly used exchange functionals mimics long-range (non-dynamic) pair correlation effects in an unspecified way [33,34]. On the contrary, if system-specific non-dynamic correlation effects are introduced via the form of the wave function as in BS-UDFT calculations through spin projection, these effects will be suppressed if the exchange functional already covers a considerable amount of non-dynamic correlation. Thus, the application of spin projection techniques to DFT calculations results then probably in the suppression (or double counting) of such long-range correlation effects.

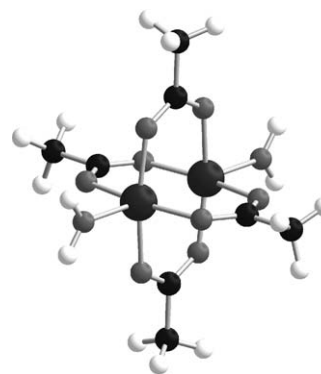
In order to illustrate the performance of the different methods commonly used to calculate exchange coupling constants we present in Table 1 the values for the exchange coupling constant calculated for the hypothetical  $\text{H}\cdots\text{He}\cdots\text{H}$  molecule at different geometries. This is the simplest system one can think of in which two unpaired electrons couple through a superexchange pathway. Although no experimental information exists for such compound, its small size makes it possible to perform full CI calculations and it has become a standard benchmark for the calculation of coupling constants.

These results show that the B3LYP hybrid DFT functional [35] in combination with Eq. (2a) yields the best approximation to the full CI results. Pure functionals like the local LDA [36,37] or the GGA-corrected BLYP [38,39] one tend to overestimate the value of the coupling constant. Using the UHF method in combination with Eq. (2b) gives also reasonable values for the coupling constant which are, however, somewhat lower than those obtained at the full CI level.

The same trends are found when applying this computational strategy to more complex systems like

transition metal dinuclear compounds. For these, the local density approximation gives the worst results, with a magnitude of  $J$  which is 3–5 times larger than the experimental value. The use of gradient-corrected functionals strongly reduces the calculated value of  $J$  that is, however, still strongly overestimated. The use of the hybrid B3LYP functional gives in this case again the best agreement with the experimental results. As an illustration of these findings we can compare the values obtained for the Cu(II) acetate dinuclear complex [40] (Scheme 2) using different methods with the experimental one (Table 2).

The comparison of the calculated  $J$  adopting the B3LYP functional and its experimental value for several families of dinuclear transition metal compounds with different bridges using the complete, non-modeled structure for each complex is shown in Fig. 1. The agreement between calculated and experimental data found for all these compounds allows us to believe that the use of this method in more complex cases like polynuclear compounds or extended solid state structures will also yield essentially correct values for the exchange coupling constant. It is specially important to point to the fact that in all dinuclear compounds studied so far the experimental sign of the coupling constant (negative for antiferromagnetic coupling, positive for ferromagnetic coupling) is correctly reproduced by using the B3LYP functional in combination with Eq. (2a). The results obtained using the UHF method are qualitatively



Scheme 2.

Table 1

Exchange coupling constants  $J$  ( $\text{cm}^{-1}$ ) for the  $\text{H}\cdots\text{He}\cdots\text{H}$  system at different  $\text{H}\cdots\text{He}$  distances [16,17,32]

Method	$d = 1.250 \text{ \AA}$	$d = 1.625 \text{ \AA}$	$d = 2.000 \text{ \AA}$
UHF	-3894	-420	-40
LDA	-6264	-775	-85
BLYP	-5391	-621	-69
B3LYP	-4367	-513	-57
Full CI	-4860	-544	-50

All values calculated using DFT-based methods have been obtained applying Eq. (2a), while Eq. (2b) has been used to obtain the UHF results. The full CI value corresponds directly to the singlet–triplet gap.

Table 2

Exchange coupling constants  $J$  ( $\text{cm}^{-1}$ ) for Cu(II) acetate calculated using several methods [7]

Method	$J$
UHF	-54
LDA	-1057
BLYP	-779
B3LYP	-299
Exp.	-297

All values calculated using DFT-based methods have been obtained applying Eq. (2a), while Eq. (2b) has been used to obtain the UHF results.

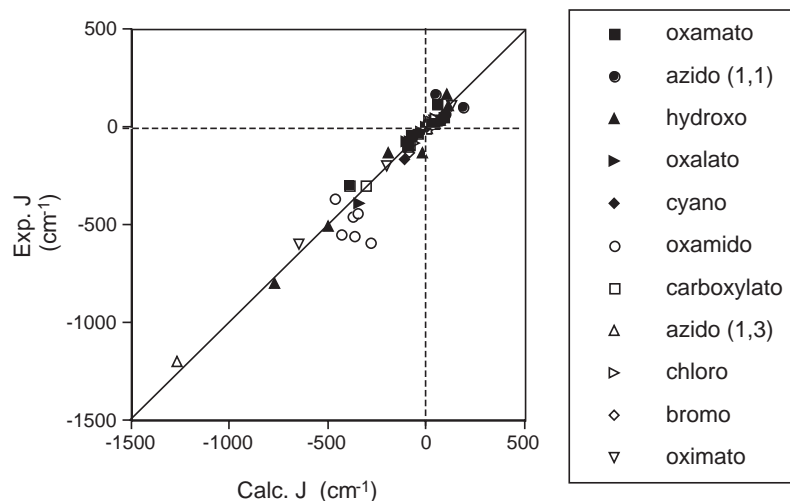


Fig. 1. Experimental exchange coupling constants for some families of dinuclear compounds with different bridging ligands, represented as a function of the calculated value with the B3LYP broken symmetry method using the complete, non-modeled structure for each compound.

correct but a significant underestimation of the value for the coupling constant is systematically found when comparing them with the experimental results.

### 3. Calculation of exchange coupling constants in extended solids

If we turn now to extended solids, the Hamiltonian usually employed is considerably more complex due to the presence of several exchange pathways with different  $J$  values. If one neglects spin–orbit coupling effects, the Hamiltonian for a general extended structure is indicated in

$$\hat{H} = \sum_{i>j} J_{ij} \hat{S}_i \hat{S}_j, \quad (3)$$

where  $\hat{S}_i$  and  $\hat{S}_j$  are the spin operators of the different paramagnetic centers. The  $J_{ij}$  values are the coupling constants between all the paramagnetic centers. The periodicity of the structure allows us to restrict ourselves to interactions within a single unit cell. In most of the cases the exchange interaction is limited only to nearest neighbors. This fact together with the presence of additional symmetry elements in the crystal structure results normally in a reduced set of  $J_{ij}$  values.

At this point it is worth to discuss about the comparability of the calculated and experimental exchange coupling constants in some detail. From the experimental point of view, the Heisenberg Hamiltonian is employed to estimate the energies of the states that are used in the fitting of the magnetic susceptibility. In the calculation of coupling constants by quantum chemical methods, the Heisenberg Hamiltonian is also adopted. When using single-determinant methods, such as DFT or HF, the calculated energies are related to the diagonal matrix elements of the Heisenberg

Hamiltonian. An alternative way to describe the system is by considering an Ising Hamiltonian as a special case of an Heisenberg Hamiltonian in which only the diagonal terms are kept. Thus, we can consider that the wavefunctions obtained with the single-determinant methods are eigenfunctions of an Ising Hamiltonian that is formulated with the same  $J$  values than the original Heisenberg Hamiltonian because their diagonal terms are identical. For that reason, the  $J$  values obtained with single-determinant methods are directly comparable to those obtained from experimental data.

The procedure proposed by us here for the calculation of the set of exchange coupling constants in an extended compound with  $n$  different  $J_{ij}$  values consists in the calculation of  $n + 1$  energies corresponding to different spin distributions within the unit cell. Such energies, as indicated above, are related to the eigenvalues of the Ising Hamiltonian (identical to the diagonal matrix elements of the Heisenberg Hamiltonian) and we can use them to obtain a system of  $n$  equations with  $n$  unknowns, the  $J_{ij}$  values.

Since for a pair of paramagnetic centers the energy difference between the ferromagnetic and the antiferromagnetic spin configurations is given by Eq. (2a), we can extend that approach to periodic extended compounds by just expressing the difference in energy between different spin configurations as a sum of pairwise interactions within the unit cell. Let us illustrate the procedure by applying it to one of the examples that will be discussed below. The crystal structure of  $\text{Ag}_2\text{Cu}_2\text{O}_3$  shown in Fig. 2 consists of alternating chains of edge-sharing square planar  $\text{CuO}_4$  units and zigzag chains of linearly coordinated silver ions [10,41].

At this stage it is only important to note that the copper atoms bearing each one unpaired electron are arranged in chains that run parallel to the  $a$  and  $b$  directions consecutively as we move along the  $c$

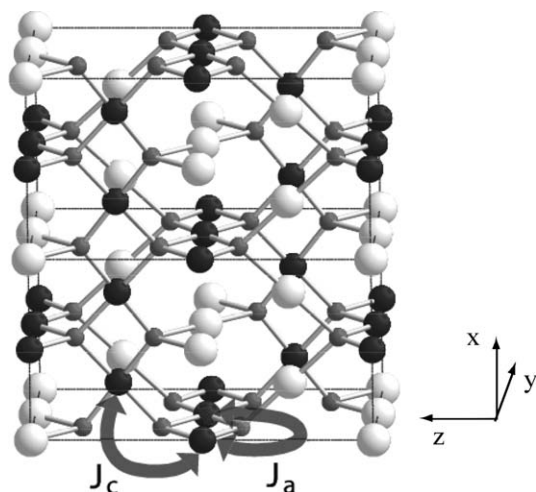


Fig. 2. Crystal structure of  $\text{Ag}_2\text{Cu}_2\text{O}_3$ . Silver, copper and oxygen atoms are represented by white, black and gray spheres, respectively.

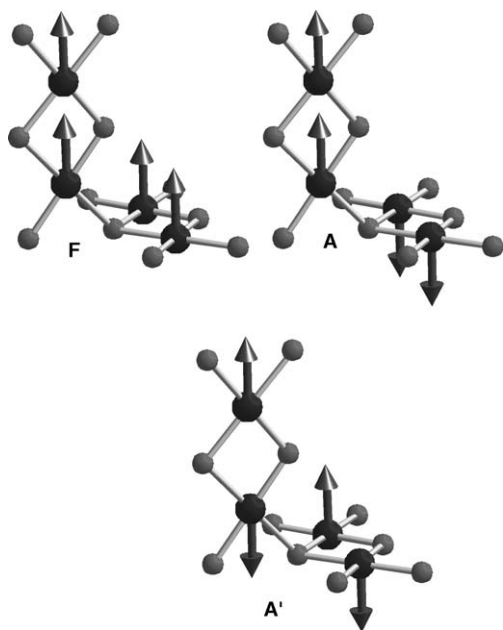


Fig. 3. Schematic representation of the three spin configurations considered to obtain the exchange coupling constants for  $\text{Ag}_2\text{Cu}_2\text{O}_3$ .

direction, resulting in a stacking of mutually perpendicular chains of  $\text{Cu}(\text{II})$  ions. In this case we can think of ferro- or antiferromagnetic coupling within and between the chains and hence, if only nearest neighbor interactions are considered, two exchange coupling constants are needed:  $J_a = J_b$  for the coupling along the chains that run parallel to the  $a$  and  $b$  directions and  $J_c$  for the interaction between neighboring perpendicular chains. In order to extract the values of these two constants we need, apart from the ferromagnetic structure (F in Fig. 3) in which all spins are aligned in the same direction, two other spin configurations. The second magnetic structure considered (A in Fig. 3) has

ferromagnetic coupling within the chains but antiferromagnetic coupling between them, while the third spin distribution considered (A' in Fig. 3) corresponds to antiferromagnetic interactions within the chains.

To extract the coupling constants from energy differences between these three spin distributions we must first determine how many interactions of each type are included in the unit cell. From the representation of the unit cell shown in Fig. 2 we can easily deduce that there are eight intrachain and 16 interchain pairs per unit cell. Since in spin distributions A and F coupling within the chains is the same, their energy difference will depend only on the intrachain coupling constant  $J_c$ :

$$E_A - E_F = 16J_c. \quad (4a)$$

The energy difference between spin distributions A' and F depends on both coupling constants. In this case all intrachain pairs and half of the interchain ones change. The energy difference between both magnetic configurations is thus

$$E_{A'} - E_F = 8J_a + 8J_c. \quad (4b)$$

From these two equations we can obtain the following expressions for the coupling constants:

$$J_c = \frac{E_A - E_F}{16} \quad (5a)$$

and

$$J_a = -\frac{1}{8} \left( \frac{E_A + E_F}{2} - E_{A'} \right). \quad (5b)$$

This approach can, in principle, be applied to any periodic structure and the difficulty of computing exchange coupling constants is only limited by the complexity of the magnetic structure of the solid. In systems with low symmetry the necessity of using a large set of coupling constants makes the procedure more tedious. In some cases it is necessary to use unit cells larger than the primitive one. The computational cost associated with the use of these supercells represents in some cases an important limitation to the application of this procedure.

#### 4. Calculation of exchange coupling constants: examples

Before describing in more detail the calculation of exchange coupling constants for some of the compounds studied in our group we would like to do a brief review of the work performed by other research groups in the same direction. The first studies of open-shell transition-metal compounds using the CRYSTAL code date back to 1993 when the possibility of performing unrestricted Hartree–Fock calculations was included in the program [22]. These early studies were devoted to simple oxides like VO, MnO or NiO [42–45]. Due to their highly symmetric rock-salt structure, these solids are relatively

simple to study, but do not give information on more subtle questions such as the influence of bond angles on superexchange and magnetic properties. Although no coupling constants were evaluated in these works, a qualitatively correct ground-state electronic structure was obtained in which the wide band-gap insulating character was found to be a result of large on-site Coulomb interactions. The effect of exchange and correlation on the bulk properties of NiO and CoO has also been examined recently performing calculations with different DFT-based methods [46].

The electronic structure of transition-metal oxides with the corundum structure has also been analyzed using the UHF method. Calculations for  $\alpha$ -Fe<sub>2</sub>O<sub>3</sub> [47], Cr<sub>2</sub>O<sub>3</sub> [48], Ti<sub>2</sub>O<sub>3</sub> and V<sub>2</sub>O<sub>3</sub> [49] predict the correct antiferromagnetic structure for  $\alpha$ -Fe<sub>2</sub>O<sub>3</sub>, Cr<sub>2</sub>O<sub>3</sub> and Ti<sub>2</sub>O<sub>3</sub>. V<sub>2</sub>O<sub>3</sub> is also predicted to be an antiferromagnetic insulator although it is experimentally found to be a metallic conductor. In the case of Ti<sub>2</sub>O<sub>3</sub> and V<sub>2</sub>O<sub>3</sub> the evolution of the magnetic properties with the  $c/a$  ratio has also been studied and an explanation for the insulator to metal transition observed in Ti<sub>2</sub>O<sub>3</sub> is given.

Other transition-metal compounds for which the magnetic properties have been studied using UHF approach within the CRYSTAL program are the antiferromagnetic MnCr<sub>2</sub>O<sub>4</sub> spinel [50], the CaMnO<sub>3</sub> and LaMnO<sub>3</sub> perovskites [51–53], MnFe<sub>2</sub>O<sub>4</sub> [54],  $\alpha$ -MnS [55,56], the cubic and hexagonal forms of  $\beta$ -MnS [56,57], pyrite-type p-MnS<sub>2</sub> [58], bimetallic Cr(III) cyanides [59], V-doped TiO<sub>2</sub> [60] and the non-cubic Mn<sub>3</sub>O<sub>4</sub> spinel [9]. In some of these cases exchange coupling constants were also estimated. For CaMnO<sub>3</sub> [51] the antiferromagnetic state is found to be more stable than the ferromagnetic one. The experimental superexchange magnetic constant can be related to the difference in energy between those two states,  $\Delta E$ , through the following relation:

$$\Delta E = z|J|S^2, \quad (6)$$

if the Ising Hamiltonian is assumed. In the above equation  $z$  is the number of Mn–Mn next-nearest neighbors and  $S$  the spin of the Mn ion. The calculated value for the exchange coupling constant,  $J_{\text{calc}} = -49$  K turns out to be about five times larger than the experimental one  $J_{\text{exp}} = -9.2$  K, where, as it is customary in solid state physics, the exchange constants in energy units have been divided by Boltzmann's constant to yield quantities with the dimensions of temperature (1 K is equivalent to  $0.695 \text{ cm}^{-1}$ ). This disagreement is probably originated by the modeling of the unit cell used in the calculations, since, as it has been found now in numerous examples, the UHF method tends to underestimate the coupling constants. Another case for which coupling constants have been calculated is the non-cubic Mn<sub>3</sub>O<sub>4</sub> spinel hausmannite [9]. From the point of view of *ab initio* calculations this case should be considered as a difficult system for various reasons: (a) it has a

tetragonally distorted spinel structure with a relatively low symmetry, (b) it contains six manganese atoms in the unit cell from which two are expected to have an electronic configuration close to  $d^5$  (Mn<sub>A</sub>) and the other four close to  $d^4$  (Mn<sub>B</sub>) and (c) the latter atoms are expected to give raise to a Jahn–Teller distortion. As far as their magnetic properties are concerned, spinels are well known for their ferrimagnetism, mainly due to antiferromagnetic interactions between the A–B sublattices. The A–A interactions are usually very weak because tetrahedra are not directly connected and B–B interactions are weaker than the A–B ones but control the B sublattice magnetic configuration. Chartier et al. [9] have used seven different spin configurations to extract, using the procedure explained in the preceding section, four different superexchange constants. Their results agree qualitatively well with the experimentally known constants, but the magnitude of the calculated coupling constants is only about 40–50% of the experimental ones.

The calculation of exchange coupling constants has been one of the main focuses of several works dedicated to solids like perovskites  $KMF_3$  ( $M = \text{Mn(II), Fe(II), Co(II) and Ni(II)}$ ) [61,62], the Jahn–Teller distorted perovskite  $KCuF_3$  [63], layered perovskites  $K_2MnF_4$  and  $K_2NiF_4$  [64], the rutile-type compounds  $MF_2$  ( $M = \text{Mn(II), Fe(II), Co(II) and Ni(II)}$ ) [65–68] or compounds related to the high  $T_c$  superconducting cuprates like  $La_2CuO_4$  and  $La_2NiO_4$  [69],  $Sr_2CuO_3$  and  $Sr_2CuO_2Cl_2$  [70],  $Li_2CuO_2$  [15] and  $CaCuO_2$  [71]. The general finding in all these works is that UHF calculations reproduce correctly the antiferromagnetic nature of the ground state but lead to values for the coupling constants which are about 30–50% of the experimental ones. In only one of these works [71] spin-polarized DFT calculations based on the B3LYP functional have been employed. The calculated electronic structure of  $CaCuO_2$  corresponds to that of an antiferromagnetic insulator for which the theoretical energy gap and magnetic moment are in excellent agreement with the experiments. The ratio of intralayer to interlayer magnetic coupling constants and lattice parameters are also in good accordance with the experiments.

As a summary of the preceding discussion we can state that the CRYSTAL program can be considered as a valuable theoretical tool for the study of magnetic properties for open-shell transition metal compounds. The UHF approach applied to a wide variety of such materials has been able in most of the cases to yield the correct magnetic structure for them. As far as exchange coupling constants are concerned the results obtained are, in general, in qualitative agreement with the experimental ones although the actual values of these parameters are strongly underestimated by the UHF approach. As discussed above, previous work performed

for dinuclear and polynuclear transition-metal compounds shows however that this trend can be overcome in most cases by using DFT-based calculations adopting the hybrid B3LYP functional. In the following we will show that this approach, which has been successfully applied for molecular compounds, can also be applied to extended solid state compounds. For this purpose we will describe with some detail some of the results obtained recently in our research group.

## 5. Exchange coupling in CuGeO<sub>3</sub>

The spin-Peierls transition is an interesting phenomenon predicted to appear in spin chains. In systems showing this type of behavior below a critical temperature a structural distortion, a dimerization of the chains, results in a rapid drop of the magnetic susceptibility. Since 1993 when CuGeO<sub>3</sub>, the first inorganic spin-Peierls compound [72], was discovered a huge amount of work has been devoted to its special magnetic properties [73]. Above 14 K CuGeO<sub>3</sub> has an orthorhombic unit cell (Fig. 4) in which linear chains of Cu(II) ions coordinated by oxygen atoms in a square planar fashion run parallel to the crystal *c* direction. The oxygen atoms bridging two copper atoms are simultaneously forming tetrahedral GeO<sub>4</sub> units that provide a link between neighboring chains in the *b* direction. At lower temperatures the unit cell is slightly distorted to give a dimer character to the chains.

From the magnetic point of view, the high temperature phase shows long-range-order antiferromagnetic coupling along the copper chains. This coupling is usually described using a Heisenberg Hamiltonian with two exchange constants  $J_c$  (between neighboring copper atoms) and  $\alpha J_c$  (between next-nearest neighbors). Depending on the experimental data different values

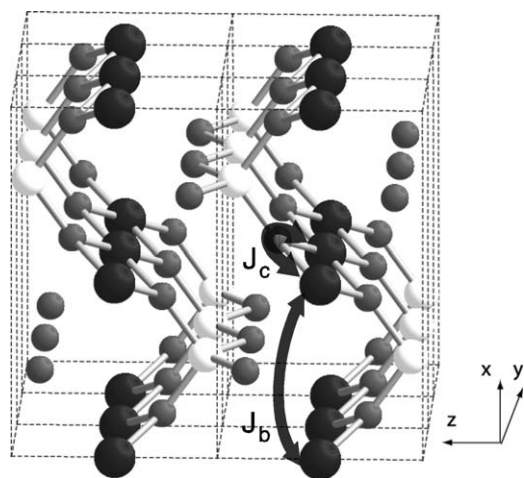


Fig. 4. Crystal structure of CuGeO<sub>3</sub>. Copper, germanium and oxygen atoms are represented by black, white and gray spheres, respectively.

have been given for  $J_c$  ranging between  $-120$  and  $-180$  K [74–78]. The value of  $\alpha$  has been estimated between 0.24 and 0.36. Coupling along the two other crystallographic directions is estimated to be much smaller ( $J_b = 0.1J_c$  and  $J_a = -0.01J_c$ ) and is usually not considered in the models employed to interpret the magnetic data of this compound.

Although several theoretical studies of the electronic structure of CuGeO<sub>3</sub> have been reported, no *ab initio* determination of the coupling constants has been attempted for the full crystal structure. In a previous paper we calculated the exchange coupling constants for this material using discrete cluster models in combination with the DFT method outlined above [79]. The two models used for this purpose included two and three copper atoms, respectively, bridged by GeO<sub>4</sub> groups. The dangling bonds at the terminal oxygen atoms were saturated using hydrogen atoms. Using the experimental geometry in the high-temperature phase our calculations for the trinuclear cluster model yield  $J_c = -154$  K and  $\alpha = 0.17$  (i.e.,  $\alpha J_c = -26$  K).<sup>1</sup> Although these results are in good agreement with the experimental data, we would like to have an estimate of the error committed by employing a finite cluster model in the calculation. This question is especially relevant if we consider that using the cluster with only two copper atoms a substantially lower value,  $-60$  K, is obtained for  $J_c$ .

Now we have undertaken the calculation of the coupling constant  $J_c$  using the full periodic crystal structure to avoid possible artifacts in the calculation due to the modeling process. In addition, the calculation for the periodic model will allow us to obtain an estimate for the intrachain coupling constant  $J_b$  which was not considered in our previous study. This case, for which more or less reliable experimental information on the coupling constants is available, represents also an excellent benchmark for testing the use of different functionals in the estimation of coupling constants for periodic structures. For the calculation of the two constants involved we have considered the three magnetic configurations sketched in Fig. 5.

The resulting equations for the coupling constants in this case are

$$J_c = \frac{E_F - E_A}{4} \quad (7a)$$

and

$$J_b = \frac{E_F - E_A'}{4} \quad (7b)$$

The values for the coupling constants obtained using different methods are presented in Table 3. A look at these results shows clearly that, for this case, the B3LYP

<sup>1</sup>The values for the exchange coupling constant for the trinuclear model in Ref. [79] are slightly different from the ones given here because they were obtained using an approximate model.

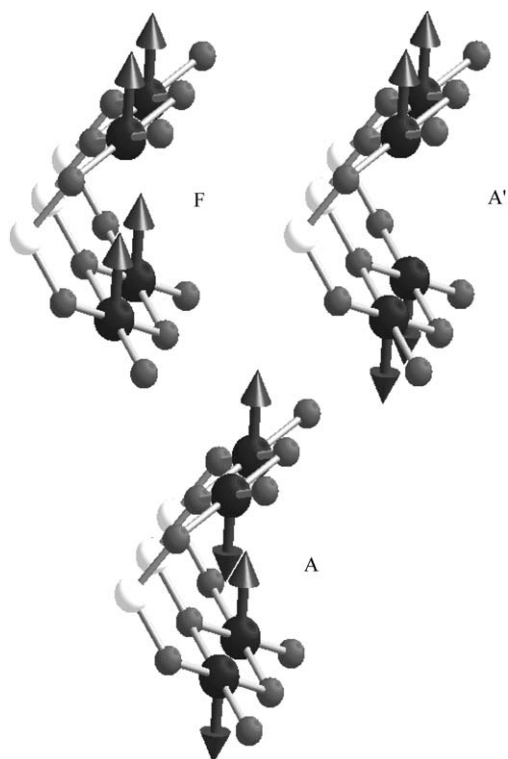


Fig. 5. Schematic representation of the three spin configurations considered to obtain the exchange coupling constants for  $\text{CuGeO}_3$ .

Table 3  
Exchange coupling constants  $J$  (K) and spin densities on the copper atoms  $\rho_{\text{Cu}}$  calculated for  $\text{CuGeO}_3$  using several methods

	$J_c$	$J_b$	$\rho_{\text{Cu}}$
UHF	+43.8	-11.2	0.92
LDA	-995.6	-490.0	0.18
BLYP	-1961.0	-115.4	0.31
B3LYP	-142.7	-10.4	0.67
Exp.	-120 to -180	-12 to -18	0.7

Hartree–Fock values calculated employing Eq. (2b) for the pairwise interaction.

method is the only one capable of reproducing the experimental data. When comparing the value of  $J_c$  with those obtained previously for cluster models we find an intermediate value which is in better agreement with the available experimental data than those found for the cluster models. Both the sign and the magnitude of the interchain coupling constant  $J_b$  agree also well with the available experimental data. The UHF method yields in this case an intrachain coupling constant with the wrong sign because the ground state is incorrectly predicted to correspond to the  $A'$  spin configuration. Calculations with pure functionals reproduce the sign of the coupling constants, but tend, as indicated above, to overestimate their magnitude. In this case the performance of the GGA-corrected functional BLYP is especially bad overestimating the coupling constants

by an order of magnitude. Despite this failure, the ratio between both constants is more or less well reproduced. For LDA calculations we find also a significant overestimation of both coupling constants and in this case the problem is especially evident for the interchain coupling constant whose value is predicted to be practically half of the intrachain one in clear contradiction with experimental results.

One important difference that arises when comparing the results obtained using the four methods concerns the delocalization of the unpaired electrons [80]. When comparing the calculated spin densities on the copper atoms it is evident that calculations using pure functionals lead to an excessively delocalized solution with spin densities as low as  $0.18e$  for the LDA case. This exaggerated delocalization is in the origin of the overestimation of the exchange coupling constants obtained when employing these methods. As found in previous work for molecular systems the UHF spin density tends to be much more localized than the DFT ones. The value obtained for the B3LYP case is in excellent agreement with the available experimental data [81].

## 6. Magnetic properties of the first silver copper oxide $\text{Ag}_2\text{Cu}_2\text{O}_3$

Although copper and silver belong to the same family, share common features, and readily form alloys in their metallic states, the formation of ternary compounds including these two elements is quite rare. In this respect, the first known silver copper oxide,  $\text{Ag}_2\text{Cu}_2\text{O}_3$ , has been synthesized recently by Gómez-Romero et al. [10,41] After a preliminary report on its synthesis and crystal structure, a detailed study of some of its physical properties including magnetic properties was published. This work presents the combined theoretical and experimental study that will be summarized here as an illustration of the calculation of exchange coupling constants using CRYSTAL to perform B3LYP spin polarized electronic structure calculations for periodic systems.

The variation of the molar magnetic susceptibility with the temperature at 10 kG was measured for  $\text{Ag}_2\text{Cu}_2\text{O}_3$ . The curve showed that the susceptibility ( $5.9 \times 10^{-4} \text{ cm}^3 \text{ mol}^{-1}$  at 290 K) increased upon cooling, reaching a broad maximum at ca. 80 K ( $\chi = 7.1 \times 10^{-4} \text{ cm}^3 \text{ mol}^{-1}$ ). Below this temperature an abrupt drop of the magnetic molar susceptibility is observed. The position of the maximum, together with the continuous decrease in the  $\chi T$  values is indicative of the antiferromagnetic behavior of the compound. As discussed above, from the crystal structure (Fig. 2) one should expect important superexchange interactions through the oxo bridges to arise both along the chains



(crystallographic  $a$  and  $b$  directions and between them (crystallographic  $c$  direction. Interactions through the Ag ions can be neglected in a first approximation. Although there are no models available for extracting exchange coupling constants from susceptibility data for three-dimensional compounds, a semiquantitative approach was adopted in which a mean field corrected chain model was employed in which interchain coupling is considered. The best fit of the experimental data to this model gives  $J_a = -77.3$  K and  $J_c = -32.2$  K for the intra- and interchain interactions, respectively. In the fitting procedure only data obtained above 85 K were considered because the model is not valid for long-range ordered magnetic states which could be involved in the susceptibility drop below 75 K. Taking all these approximations into account, the exchange coupling constants obtained cannot be taken as precise numerical values but they lead to two qualitative conclusions that should be reproduced in the theoretical study: (a) the compound is moderately antiferromagnetic and (b) coupling between chains is similar in sign and magnitude to that within the chains.

Electronic structure calculations using the B3LYP functional for  $\text{Ag}_2\text{Cu}_2\text{O}_3$  and isostructural paramelacnite ( $\text{Cu}_4\text{O}_3$ ) confirm the picture obtained from experimental data. As mentioned above three magnetic configurations (Fig. 3) must be considered in this case in order to compute the two coupling constants considered. For both compounds the  $A'$  spin distribution is found to be the most stable one. By applying Eqs. (4a) and (4b) we find  $J_a = -32.5$  K,  $J_c = -32.4$  K and  $J_a = -16.0$  K,  $J_c = -14.2$  K for  $\text{Ag}_2\text{Cu}_2\text{O}_3$  and  $\text{Cu}_4\text{O}_3$ , respectively. Although in this case we do not have accurate experimental values for comparison, these calculated coupling constants are fully consistent with the conclusions obtained from experimental data showing that the theoretical calculation of the coupling constants can be a valuable tool to extract information at the microscopic level even in cases where no precise experimental information is available. For a more complete discussion on the values of the calculated coupling constants and their relation to exchange coupling constants in related molecular and solid state Cu(II) compounds the reader is addressed to the original Ref. [10].

## 7. Magnetic properties of transition metal complexes with the dicyanamide anion

One of the most recent areas of interest in molecular magnetism is the engineering of infinite metal-organic polymeric frameworks with the aim of constructing novel crystal architectures with interesting magnetic properties. A key factor in this purpose is the magnetic coupling between nearest neighbor metal-based spin

sites provided by an intermediary ligand. Except for ligands bearing unpaired electrons, the strongest coupling, in general, is expected for the ligands with the fewest atoms and the greatest conjugation. The ability of cyanide, tricyanomethanide and dicyanamide to form homoleptic compounds as well as to bridge two or more metal ions together with their highly conjugated nature has triggered in recent time an intense research effort in the synthesis and characterization of novel three-dimensional network solids with these ligands exhibiting interesting magnetic properties [82].

In this contribution we will focus on the magnetic properties of the  $M[\text{N}(\text{CN})_2]_2$  ( $M = \text{V}(\text{II}), \text{Cr}(\text{II}), \text{Mn}(\text{II}), \text{Fe}(\text{II}), \text{Co}(\text{II}), \text{Ni}(\text{II})$  and  $\text{Cu}(\text{II})$ ) series of homoleptic transition metal compounds obtained with the dicyanamide ion [83,84]. Experimental studies show that with the exception of the Cu compound [83], which behaves as a paramagnet, all other show spontaneous magnetization and have well-defined hysteresis loops below their Curie temperatures which can be as high as 47 K ( $M = \text{Cr}(\text{II})$ ) [85]. Detailed studies show that  $M[\text{N}(\text{CN})_2]_2$  ( $M = \text{Co}(\text{II}), \text{Ni}(\text{II})$ ) [86] behave as ferromagnets while  $M[\text{N}(\text{CN})_2]_2$  ( $M = \text{V}(\text{II}), \text{Cr}(\text{II}), \text{Mn}(\text{II})$  and  $\text{Fe}(\text{II})$ ) order as weak ferromagnets (or canted antiferromagnets) [82,85,87]. It is also interesting to note that the Fe compound has the largest coercive field (17800 Oe) of all known metal-organic magnets and even larger than alloys containing rare-earth elements such as  $\text{SmCo}_5$  or  $\text{Nd}_2\text{Fe}_{14}\text{B}$  [83].

Since despite of forming an isostructural series there is a considerable variation in the magnetic properties of these compounds we found it interesting to analyze the metal–metal exchange coupling interactions in them using electronic structure calculations. The crystal structures of  $M[\text{N}(\text{CN})_2]_2$  are based on close packing of linear ribbons that propagate along the crystallographic  $c$  direction (Fig. 6). Within these ribbons (Fig. 6 top) the dicyanamide ions form double bridges between neighboring metal ions. Coordination of the metal atoms to the amide nitrogen atoms of adjacent chains complete the three-dimensional framework shown in Fig. 6 bottom. As can be seen in Fig. 6 the metal atoms in this structure show a pseudo-octahedral  $4+2$  coordination environment. An alternative description of the structure is to see it as a single network, isostructural to the rutile polymorph of  $\text{TiO}_2$  where  $M$  and the dicyanamide ion replace Ti and O, respectively.

From the exchange coupling point of view, in the present rutile-type structure there are four independent nearest neighbor interactions: eight equivalent superexchange  $M\text{--N--C--N--}M'$  pathways between adjacent chains with an  $M\cdots M$  separation around 5.9 Å (Fig. 6); two equivalent interactions along each of the crystallographic  $a$ - and  $b$ -axis with  $M\cdots M$  separations of about 6 and 7.1 Å, respectively; and a further two superexchange interactions along the  $c$ -axis through the

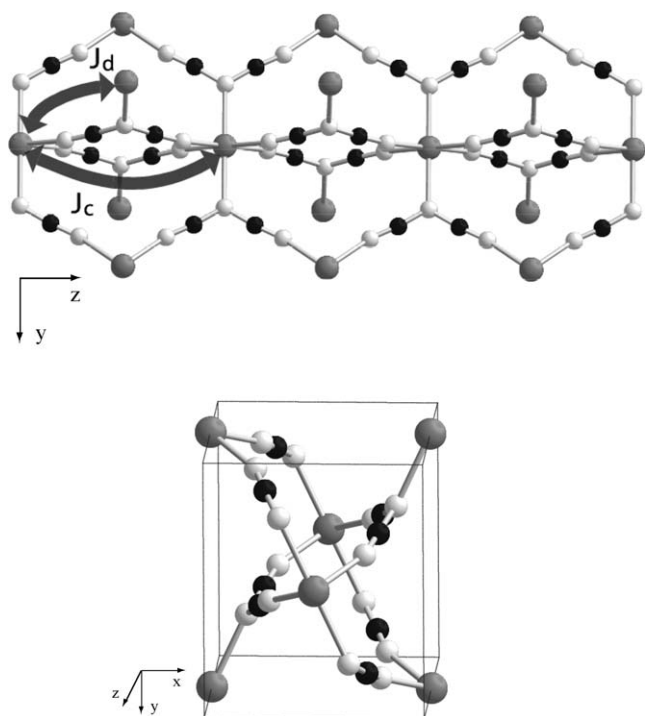


Fig. 6. Crystal structure for the series of  $M[N(CN)_2]_2$  compounds showing (top) the segment of a chain with each  $M$  atom being hexacoordinated and bridged by  $\mu_3$ - $[N(CN)_2]^-$  ions and (bottom) a view parallel to the chains. The two possible superexchange pathways for this structure are also indicated. Carbon, nitrogen and metal atoms are represented by black, white and gray spheres, respectively.

two five-atom N–C–N–C–N bridges with a  $M \cdots M$  distance around 7.3 Å (Fig. 6). Within this structure it is evident that the signs and magnitudes of the coupling constants, and hence the magnetic properties of the material, will strongly depend on fine structural details such as the  $M$ –N coordination distances and of the degree of structural distortions. The absence of a clear relationship between the metal spin state and the Curie temperatures for the different metals provides a further evidence on the dependence of the magnetic properties on structural details rather than on the metal spin state alone. The paramagnetic behavior in the copper compound is likely to arise from a severe weakening of the superexchange interaction between chains due to the Jahn–Teller distortion around the Cu(II) ion. It is further indicative that, as expected from their relatively long  $M \cdots M$  distances, all other exchange interactions in the structure must be very weak. Taking these considerations into account we will only consider in the present study the super-exchange interaction between neighboring chains mediated by the three-atom N–C–N bridges.

From the computational point of view, the calculation of the coupling constant for the interaction between adjacent chains is fairly simple in this case. Since there are only two equivalent metal atoms per unit cell, the difference between the ferromagnetic and the antiferro-

magnetic solution leads directly to the value of  $J_d$  (the  $d$  subscript indicates that this interaction is in the direction of the diagonal of the  $a$ - and  $b$ -axis of the unit cell, see Fig. 6). For the calculation of other coupling constants larger supercells are needed.

The calculated coupling constants for the  $M[N(CN)_2]_2$  ( $M$  = Cr(II), Mn(II), Fe(II), Co(II), Ni(II) and Cu(II)) series of compounds using the B3LYP functional are shown in Table 4 together with the experimentally observed magnetic behavior and ordering temperatures. Taking into account that a simplified model with collinear spins is adopted in our calculations, the calculated results are in good qualitative agreement with the available experimental information except for the case of the Fe compound. For  $M$  = Co(II) and Ni(II) ferromagnetic coupling is predicted and the relative magnitude of the coupling constants agrees well with the observed ordering temperatures which indicate a higher value of  $T_c$  for the stronger coupling predicted for the nickel compound. The same behavior is found for compounds containing Cr(II) and Mn(II) where the higher ordering temperature corresponds to the compound for which the stronger coupling (antiferromagnetic in this case) is predicted. The almost negligible coupling constant calculated for the copper compound is also in good agreement with the paramagnetic behavior observed for  $Cu[N(CN)_2]_2$ .

The case of the Fe compound poses an extremely difficult problem to the computational approach to determine the coupling constants. In the relatively weak, pseudo-octahedral ligand field the  $3d^6$  electronic configuration is expected to give rise to the  $^5T_{2g}$  state. With two unpaired electrons in the  $t_{2g}$  orbitals and two in the  $e_g$  ones there will be an equivalent number of antiferromagnetic and ferromagnetic interactions, with the total coupling resulting from a subtle balance between these four interactions. In addition, spin–orbit coupling effects, which are large for the Fe(II) compound have neither been taken into account in these calculations.

Table 4

Exchange coupling constants  $J_d$  (K) calculated for the  $M[N(CN)_2]_2$  series of compounds using the B3LYP functional

M(II)	$J_d$	Observed behavior	$T_c$
Cr	–12.4	c-AFM	47
Mn	–1.8	c-AFM	16
Fe	+0.1	c-AFM	18
Co	+1.9 (+0.6)	FM	9
Ni	+3.2 (+2.0)	FM	21
Cu	+0.1	CW	—

Values in parentheses correspond to the mean-field result for  $J_d$  given in Ref. [87]. Experimentally observed magnetic behavior (FM = ferromagnetic, c-AFM = canted antiferromagnetic, CW = Curie–Weiss behavior) and ordering temperatures  $T_c$  (K) are also indicated [83,84,86,87].

As a conclusion, we can state that calculation of the exchange coupling constant for the three-atom N–C–N path in this family of compounds provides a reasonable explanation of the properties for all the compounds in the series with the exception of  $\text{Fe}[\text{N}(\text{CN})_2]_2$ . Since the alternative superexchange path  $J_c$  through five-atom N–C–N–C–N bridges may play also a significant role in the magnetic properties of these compounds, current investigations in our group are being carried out performing calculations using a doubled supercell in order to be able to evaluate the relative magnitude of the coupling constant for this alternative path.

## 8. Conclusions

The three examples presented in this communication show that the evaluation of exchange coupling constants for relatively complex solids containing open-shell transition metal ions can be used as a valuable and reliable source of information for the interpretation of their magnetic properties. The implementation of the computational tools that are required for this task in a standard program like CRYSTAL opens the possibility of calculating these parameters to any researcher in the field. It should be, however, reminded that the calculations described above are in no way easy, routine calculations and that they can become very time consuming, especially in the case in which the use of supercells is needed to extract the whole set of coupling constants.

## Acknowledgments

Financial support came from *Direcció General de Investigació (DGI)* through project number BQU2002-04033-C02-02 and from *Comissió Interdepartamental de Ciència i Tecnologia (CIRIT)* through grant 2001SGR-0044. The computing resources at *CESCA/CEPBA-CIRI* were generously made available through grants from *CIRIT, Universitat de Barcelona* and *CEPBA-IBM Research Institut*.

## Appendix A. Computational details

The evaluations of exchange coupling constants presented in this work has been performed via density functional calculations using the CRYSTAL-98 package [22] with the B3LYP combination of exchange and correlation functionals. In all calculations for the evaluation of the Coulomb and exchange integrals tolerance factors of 7, 7, 7, 7 and 14 were used and the convergence criterion for the energy set to  $10^{-7}$  a.u.

[88,89]. Specific details for each of the systems studied are as follows:

$\text{Ag}_2\text{Cu}_2\text{O}_3$  and  $\text{Cu}_4\text{O}_3$ : A triple- $\zeta$  quality basis set of gaussian-type functions including polarization functions was used in the calculations for copper and oxygen atoms while a double- $\zeta$  basis set was employed for silver atoms. The contraction schemes adopted are (633311/53211/531) for the silver atoms, (632111/33111/311) for the copper atoms and (8411/411/1) for the oxygen atoms. Integration of k-dependent magnitudes in the reciprocal space was carried out using a mesh of 46 k-points for the F and A states and of 68 k-points for the A' one.

$\text{CuGeO}_3$ : A triple- $\zeta$  basis set with a polarization function was employed with a contraction scheme (632111/33111/311) for the copper atoms, (8411/411/1) for the oxygen atoms and (97631/7631/61) for the germanium atoms. A total of 170 k-points were employed to perform the integration of the k-dependent magnitudes in the reciprocal space.

$M[\text{N}(\text{CN})_2]_2$ : For the metal atoms, we have employed a double- $\zeta$  basis set with a contraction scheme (86411/6411/41) while for carbon and nitrogen atoms a 6-21G basis set was used. Although a smaller basis set is used for this family of compounds, previous work on molecular compounds [19] has shown that it is sufficient to reproduce the coupling constants at a qualitative level. A mesh of 80 k-points was employed for the integration in the reciprocal space.

## References

- [1] O. Kahn, *Molecular Magnetism*, VCH Publishers, New York, 1993.
- [2] J.S. Miller, M. Drillon (Eds.), *Magnetism: Molecules to Materials Molecule-based Materials*, Wiley-VCH, Weinheim, 2001.
- [3] J.S. Miller, M. Drillon (Eds.), *Magnetism: Molecules to Materials Models and Experiments*, Wiley-VCH, Weinheim, 2001.
- [4] J.S. Miller, M. Drillon (Eds.), *Magnetism: Molecules to Materials Nanosized Magnetic Materials*, Wiley-VCH, Weinheim, 2002.
- [5] O. Kahn, Y. Pei, Y. Journaux, in: Q.W. Bruce, D. O'Hare (Eds.), *Inorganic Materials*, Wiley, Chichester, 1992, p. 59.
- [6] L. Néel, *Ann. Phys. Paris* 3 (1948) 137.
- [7] E. Ruiz, S. Alvarez, A. Rodríguez-Forteza, P. Alemany, Y. Pouillon, C. Massobrio, in: J.S. Miller, M. Drillon (Eds.), *Magnetism: Molecules to Materials Molecule-based Materials*, Wiley-VCH, Weinheim, 2001, p. 227.
- [8] E. Ruiz, A. Rodríguez-Forteza, P. Alemany, S. Alvarez, *Polyhedron* 20 (2001) 1323.
- [9] A. Chartier, P. D'Arco, R. Dovesi, V.R. Saunders, *Phys. Rev. B* 60 (1999) 14042.
- [10] E.M. Tejada-Rosales, J. Rodríguez-Carvajal, N. Casañ-Pastor, P. Alemany, E. Ruiz, M. Salah El-Fallah, S. Alvarez, P. Gómez-Romero, *Inorg. Chem.* 41 (2002) 6604.
- [11] F. Jensen, *Introduction to Computational Chemistry*, Wiley, Chichester, 1999.
- [12] K. Fink, C. Wang, V. Staemmler, *Inorg. Chem.* 38 (1999) 3847.
- [13] A. Ceulemans, L.F. Chibotaru, G.A. Heylen, K. Pierloot, L.G. Vanquickenborne, *Chem. Rev.* 100 (2000) 787.

- [14] O. Castell, R. Caballol, *Inorg. Chem.* 38 (1999) 668.
- [15] C. de Graaf, I.d.P.R. Moreira, F. Illas, O. Iglesias, A. Labarta, *Phys. Rev. B* 66 (2002) 014448.
- [16] R. Caballol, O. Castell, F. Illas, I.d.P.R. Moreira, J.P. Malrieu, *J. Phys. Chem. A* 101 (1997) 7860.
- [17] E. Ruiz, J. Cano, S. Alvarez, P. Alemany, *J. Comp. Chem.* 20 (1999) 1391.
- [18] W. Koch, M.C. Holthausen, *A Chemist's Guide to Density Functional Theory*, Wiley-VCH Verlag, Weinheim, 2000.
- [19] E. Ruiz, P. Alemany, S. Alvarez, J. Cano, *J. Am. Chem. Soc.* 119 (1997) 1297.
- [20] E. Ruiz, P. Alemany, S. Alvarez, J. Cano, *Inorg. Chem.* 36 (1997) 3683.
- [21] E. Ruiz, J. Cano, S. Alvarez, P. Alemany, *J. Am. Chem. Soc.* 120 (1998) 11122.
- [22] V.R. Saunders, R. Dovesi, C. Roetti, M. Causà, N.M. Harrison, R. Orlando, C.M. Zicovich-Wilson, *CRYSTAL98*, University of Torino, Torino, 1998.
- [23] G.S. Rushbrooke, P.J. Wood, *Mol. Phys.* 1 (1958) 257.
- [24] J. Cano, P. Alemany, S. Alvarez, M. Verdaguer, E. Ruiz, *Chem. Eur. J.* 4 (1998) 476.
- [25] J. Cano, A. Rodríguez-Fortea, P. Alemany, S. Alvarez, E. Ruiz, *Chem. Eur. J.* 6 (2000) 327.
- [26] A. Rodríguez-Fortea, P. Alemany, S. Alvarez, E. Ruiz, *Chem. Eur. J.* 7 (2001) 627.
- [27] E. Ruiz, S. Alvarez, P. Alemany, *Chem. Commun.* (1998) 2767.
- [28] C. Desplanches, E. Ruiz, A. Rodríguez-Fortea, S. Alvarez, *J. Am. Chem. Soc.* 124 (2002) 5197.
- [29] L. Noodleman, *J. Chem. Phys.* 74 (1981) 5737.
- [30] L. Noodleman, D.A. Case, *Adv. Inorg. Chem.* 38 (1992) 423.
- [31] L. Noodleman, C.Y. Peng, D.A. Case, J.M. Mouesca, *Coord. Chem. Rev.* 144 (1995) 199.
- [32] A. Bencini, F. Totti, C.A. Daul, K. Doclo, P. Fantucci, V. Barone, *Inorg. Chem.* 36 (1997) 5022.
- [33] J. Gräfenstein, A.M. Hjerpe, E. Kraka, D. Cremer, *J. Phys. Chem. A* 104 (2000) 1748.
- [34] V. Polo, E. Kraka, D. Cremer, *Theor. Chem. Acc.* 107 (2002) 291.
- [35] A.D. Becke, *J. Chem. Phys.* 98 (1993) 5648.
- [36] J.C. Slater, *The Self-Consistent Field for Molecules and Solids*, McGraw-Hill, New York, 1974.
- [37] S.H. Vosko, L. Wilk, M. Nusair, *Can. J. Phys.* 58 (1980) 1200.
- [38] A.D. Becke, *Phys. Rev. A* 38 (1988) 3098.
- [39] C. Lee, W. Yang, R.G. Parr, *Phys. Rev. B* 37 (1988) 785.
- [40] B. Bleaney, K.D. Bowers, *Proc. Roy. Soc. (London) Ser. A* 214 (1952) 451.
- [41] P. Gómez-Romero, E.M. Tejada-Rosales, M.R. Palacín, *Angew. Chem. Int. Ed.* 38 (1999) 524.
- [42] M.D. Towler, N.L. Allan, N.M. Harrison, V.R. Saunders, W.C. Mackrodt, E. Aprà, *Phys. Rev. B* 50 (1994) 5041.
- [43] M.D. Towler, N.L. Allan, N.M. Harrison, V.R. Saunders, W.C. Mackrodt, *J. Phys.: Condens. Matter* 7 (1995) 6231.
- [44] W.C. Mackrodt, N.M. Harrison, V.R. Saunders, N.L. Allan, M.D. Towler, E. Aprà, R. Dovesi, *Philos. Mag. A* 68 (1993) 653.
- [45] W.C. Mackrodt, E.-A. Williamson, *J. Phys.: Condens. Matter* 9 (1997) 6591.
- [46] T. Bredow, A.R. Gerson, *Phys. Rev. B* 61 (2000) 5194.
- [47] M. Catti, G. Valerio, R. Dovesi, *Phys. Rev. B* 51 (1995) 7441.
- [48] M. Catti, G. Sandrone, G. Valerio, R. Dovesi, *J. Phys. Chem. Solids* 57 (1996) 1735.
- [49] M. Catti, G. Sandrone, R. Dovesi, *Phys. Rev. B* 55 (1997) 16122.
- [50] F. Freyria Fava, I. Baraille, A. Lichanot, C. Larrieu, R. Dovesi, *J. Phys.: Condens. Matter* 9 (1997) 10715.
- [51] F. Freyria Fava, P. D'Arco, R. Orlando, R. Dovesi, *J. Phys.: Condens. Matter* 9 (1997) 489.
- [52] M. Nicastro, M. Kuzmin, C.H. Patterson, *Comput. Mater. Sci.* 17 (2000) 445.
- [53] Y.-S. Su, T.A. Kaplan, S.D. Mahanti, J.F. Harrison, *Phys. Rev. B* 61 (2000) 1324.
- [54] W.C. Mackrodt, E.-A. Simson, *Faraday Trans.* 92 (1996) 2043.
- [55] R. Tappero, P. D'Arco, A. Lichanot, *Chem. Phys. Lett.* 273 (1997) 83.
- [56] R. Tappero, P. Wolfers, A. Lichanot, *Chem. Phys. Lett.* 335 (2001) 449.
- [57] R.I. Hines, N.L. Allan, G.S. Bell, W.C. Mackrodt, *J. Phys.: Condens. Matter* 9 (1997) 7105.
- [58] R. Tappero, I. Baraille, A. Lichanot, *Phys. Rev. B* 58 (1998) 1236.
- [59] N.M. Harrison, B.G. Searle, E.A. Seddon, *Chem. Phys. Lett.* 266 (1997) 507.
- [60] R.A. Evarestov, V.P. Smirnov, *Phys. Stat. Sol. B* 215 (1999) 949.
- [61] R. Dovesi, F. Freyria Fava, C. Roetti, V.R. Saunders, *Faraday Discuss.* 106 (1997) 173.
- [62] J.M. Ricart, R. Dovesi, V.R. Saunders, C. Roetti, *Phys. Rev. B* 52 (1995) 2381.
- [63] M.D. Towler, R. Dovesi, V.R. Saunders, *Phys. Rev. B* 52 (1994) 10150.
- [64] R. Dovesi, J.M. Ricart, V.R. Saunders, R. Orlando, *J. Phys.: Condens. Matter* 7 (1995) 7997.
- [65] I.d.P.R. Moreira, R. Dovesi, C. Roetti, V.R. Saunders, R. Orlando, *Phys. Rev. B* 62 (2000) 7816.
- [66] P. Reinhardt, M.P. Habas, R. Dovesi, I.d.P.R. Moreira, F. Illas, *Phys. Rev. B* 59 (1999) 1016.
- [67] P. Reinhardt, I.d.P.R. Moreira, C. de Graaf, R. Dovesi, F. Illas, *Chem. Phys. Lett.* 319 (2000) 625.
- [68] G. Valerio, M. Catti, R. Dovesi, R. Orlando, *Phys. Rev. B* 52 (1995) 2422.
- [69] Y.-S. Su, T.A. Kaplan, S.D. Mahanti, J.F. Harrison, *Phys. Rev. B* 59 (1999) 10521.
- [70] W.C. Mackrodt, H.J. Gotsis, *Phys. Rev. B* 62 (2000) 10728.
- [71] X.-B. Feng, N.M. Harrison, 1 (2003) ArXiv:cond-mat/0212588.
- [72] M. Hase, I. Terasaki, K. Uchinokura, *Phys. Rev. Lett.* 70 (1993) 3651.
- [73] J.P. Boucher, L.P. Regnault, *J. Phys. I (France)* 6 (1996) 1939.
- [74] M. Nishi, O. Fujita, J. Akimitsu, *Phys. Rev. B* 50 (1994) 6508.
- [75] J. Riera, A. Dobry, *Phys. Rev. B* 51 (1995) 16098.
- [76] G. Castilla, S. Chakravarty, V.J. Emery, *Phys. Rev. Lett.* 75 (1995) 1823.
- [77] K. Fabricius, A. Klümper, U. Löw, B. Büchner, T. Lorenz, G. Dhalenne, A. Revcolevschi, *Phys. Rev. B* 57 (1998) 1102.
- [78] H. Nojiri, Y. Shimamoto, N. Miura, M. Hase, K. Uchinokura, H. Kojima, I. Tanaka, Y. Shibuya, *Phys. Rev. B* 52 (1995) 12749.
- [79] E. Ruiz, J. Cano, S. Alvarez, P. Alemany, M. Verdaguer, *Phys. Rev. B* 61 (2000) 54.
- [80] J. Cano, E. Ruiz, S. Alvarez, M. Verdaguer, *Comments Inorg. Chem.* 20 (1998) 27.
- [81] G.A. Petrakovski, K.A. Sablina, A.M. Vorotynov, A.I. Kruglik, A.G. Klimenko, A.D. Balayev, S.S. Aplesnin, *Zh. Eksp. Teor. Fiz.* 98 (1990) 1382 (Engl. Transl. *Sov. Phys.-JETP* 71 (1990) 772).
- [82] J.S. Miller, J.L. Manson, *Acc. Chem. Res.* 34 (2001) 563.
- [83] M. Kurmoo, C.J. Kepert, *New J. Chem.* (1998) 1515.
- [84] S.R. Batten, P. Jensen, B. Moubaraki, K.S. Murray, R. Robson, *Chem. Commun.* (1998) 439.
- [85] J.L. Manson, C.R. Kmetz, A.J. Epstein, J.S. Miller, *Inorg. Chem.* 38 (1999) 2552.
- [86] J.L. Manson, C.R. Kmetz, Q.-Z. Huang, J.W. Lynn, G.M. Bendele, S. Pagola, P.W. Stephens, L.M. Liable-Sands, A.L. Rheingold, A.J. Epstein, J.S. Miller, *Chem. Mater.* 10 (1998) 2552.
- [87] J.L. Manson, C.R. Kmetz, F. Palacio, A.J. Epstein, J.S. Miller, *Chem. Mater.* 13 (2001) 1068.
- [88] R. Dovesi, J.M. Ricart, V.R. Saunders, R. Orlando, *J. Phys.: Condens. Matter* 7 (1995) 7997.
- [89] R. Dovesi, F. Freyria Fava, C. Roetti, V.R. Saunders, *Faraday Discuss.* 106 (1997) 189.